Role of oxygen impurities in etching of silicon by atomic hydrogen[a)]

Stan Veprek,[b)] Chunlin Wang,[c)] and Maritza G. J. Veprek-Heijman
Department of Chemistry, Technical University Munich, Lichtenbergstr. 4, D-85747 Garching, Munich, Germany

(Received 8 February 2007; accepted 29 January 2008; published 26 March 2008)

In a pure-hydrogen glow discharge plasma, the etch rate of silicon increases with increasing temperature up to about ≥ 1100 Å/s at 60–80 °C and, upon a further increase of the temperature, etch rate strongly decreases, showing Arrhenius-like dependence with negative apparent activation energy of −1.5 kcal/mol. When the Si sample is at the floating potential, oxygen impurities of ≥ 10 at. ppm strongly decrease the etch rate. At more than 70 ppm of oxygen, the etching stops. Oxygen adsorbed on the Si surface can be removed by ion bombardment when negative potential is applied to the Si sample and the Si is then etched chemically by H atoms. The etching by atomic hydrogen is isotropic in an oxygen-free system. A controllable addition of a few ppm of oxygen in combination with negative bias of the Si sample results in highly anisotropic etching with thin oxide acting as side-wall passivation. © *2008 American Vacuum Society.* [DOI: 10.1116/1.2884731]

I. INTRODUCTION

Etching and posttreatment of silicon with hydrogen glow discharge plasma[1–16] or with atomic hydrogen produced by hot filament[4,17,18] have again received significant attention recently in the context of new, alternative gases and processes for patterning in microelectronic device fabrication,[1–3] posttreatment of thin-film silicon in order to enhance its crystallization,[11–14] cleaning and passivation of wafers prior to the deposition of epitaxial films,[19–37] and cleaning of devices for controlled nuclear research[38,39] and of equipment for plasma-induced deposition of thin films.[2] The etching is also the initial step in the chemical transport of silicon, which has been used in the first report on the preparation of nanocrystalline silicon, nc-Si,[40] which is nowadays an important material for large-scale microelectronic devices such as thin-film transistors in flat-panel displays and for stable thin-film solar cells.[41,42] The present paper focuses on the etching reaction.

Plasma-induced and -assisted etching processes can be divided between chemical etching, physical sputtering, chemical sputtering, and reactive-ion etching.[43–47] The chemical etching of Si and Ge in hydrogen plasma has been described by Veprek and Marecek in conjunction with the chemical transport,[40] that of As, Sb, and Te by Ing and Chiang,[43] and "chemical sputtering" of As, Sb, Bi, C, and Te has been reported by Günterschulze.[48] The etching of phosphorus by atomic hydrogen is also the first step in the preparation of amorphous and nanocrystalline black phosphorus by chemical transport in hydrogen plasma[49] with excellent electronic properties[50] and surprisingly high stability against oxidation.[51] A simultaneous ion- or electron-bombardment usually enhances the etch rate by increasing the effective reactive-sticking coefficient of the hydrogen and enhancing the reactivity of the solid due to radiation damage, as shown, e.g., for carbon.[52] The synergistic effects of ion bombardment and chemical etching were investigated and discussed in some details by Winters and Coburn *et al.*[47]

Webb *et al.* investigated the etching of silicon in hydrogen discharge by means of *in situ* thermogravimetry.[53] With increasing temperature, the etch rate initially increased, reached a maximum at about 60 °C, and, upon a further increase of the temperature, the etch rate decreased. This decrease means a negative effective-activation energy, which is typical for complex reactions where an exothermic equilibrium precedes the rate-determining step of the product formation.[54] Therefore, Webb and Veprek suggested a reaction mechanism based on a step-wise addition of chemisorbed hydrogen to the Si-surface until volatile silane is formed. Simultaneously, heterogeneous recombination of hydrogen proceeds, resulting in depletion of the concentration of chemisorbed hydrogen. A similar mechanism has also been proposed for the electron-induced etching of silicon in hydrogen plasma.[55] Negative activation energy in the high-temperature region of −4.2 kcal/mol with a preexponential factor of 1.5×10^{-5} has been obtained from the Arrhenius plot (see Fig. 2 in Ref. 55). In both studies, the etch rate increased with the discharge-current density and with the hydrogen pressure, indicating its nearly linear dependence on the concentration of atomic hydrogen. This is in accord with the proposed mechanism of the step-wise addition of chemisorbed hydrogen, i.e., with an overall reaction $Si(s)+4H \rightarrow SiH_4$ being pseudo first order. The negative value of the effective-activation energy has been explained by a higher (positive) value of the activation energy for the heterogeneous-hydrogen recombination and desorption of H_2, as compared to that of silane formation (see Table I in Ref. 55).

Veprek and Sarott[55] also emphasized the problem of embrittlement of the silicon by hydrogen, which is in agreement with later measurements of a high concentration of hydrogen of up to 0.2 at. % in silicon wafers that were exposed to

[a)]Dedicated to Professor W. A. Herrmann, President of the Technical University of Munich, on the occasion of his 60th birthday.
[b)]Electronic mail: veprek@ch.tum.de
[c)]Present address: 8710 Glen Canyon Dr., Round Rock, TX 78681.

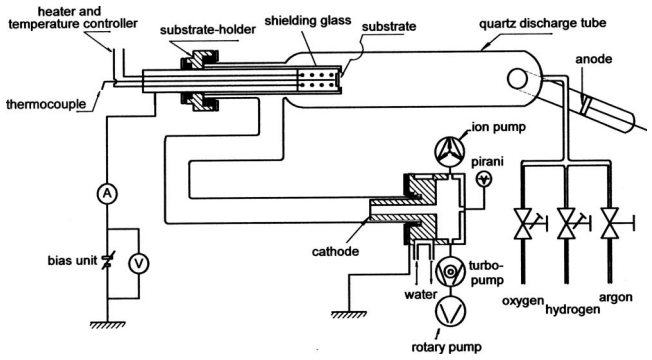

FIG. 1. Schematic drawing of the apparatus used in the present study (see text).

sources of atomic hydrogen.[56,57] Hydrogen in Si wafers can deactivate hole-bound states[58] and passivate defects.[59] In *p*-type silicon hydrogen occupies a position between the Si-Si atoms as H^+, and in *n*-type Si, H^- occupies an interstitial tetrahedral position.[60] The hydrogen embrittlement of materials exposed to hydrogen plasma is a general phenomena that has also been reported for steels,[61] titanium,[62,63] and other materials.[64]

In 1989, Abrefah and Olander used the modulated-molecular-beam technique to study the etching of Si with H atoms produced by dissociation of hydrogen in a hot tungsten tube.[65] Abrefah and Olander elaborated a detailed mechanistic model whose results are in good agreement with that of Veprek *et al.*[53,55] Gates *et al.* studied the reaction between silicon and atomic hydrogen by means of temperature-programmed desorption.[66–69]

The interaction of hydrogen with the silicon surface has often been identified to be crucial for the growth of nc-Si. Many papers quoted above report on the etching and surface treatment of Si with atomic hydrogen, but without such detailed studies. In the present paper we shall focus on the effect of oxygen on the etch rate because it has not been addressed in the recent papers. In order to provide a basis for comparison with the earlier work, we shall first describe etching in a pure-hydrogen discharge.

II. EXPERIMENT

The apparatus used in the present study (Fig. 1) consisted of a discharge tube with an inner diameter of 7.6 cm made of silica ("quartz glass"), which was connected to a remote hollow cathode via silica tubing of a diameter of 3 cm in order to avoid the back diffusion of impurities, which are usually produced in the cathode region. The dc glow discharge was maintained between the anode and the grounded hollow cathode. The 2×2 cm^2 small silicon samples were cut from an undoped Si wafer and fixed on a holder made of stainless steel, whose temperature was precisely controlled by means of electric resistance heating, a thermocouple inserted into the substrate holder (see Fig. 1), and a thermo-controller (not shown). The temperature reading of the thermocouple was also compared with that of an infrared pyrometer sensing the surface of the Si sample. The seals between the silica tube and the sample holder, as well as the cathode, were made of two Viton O-rings with the space between them being pumped to $\leq10^{-2}$ mbar. This reduced the leaks from the atmosphere by orders of magnitude. The whole system was ultra-high-vacuum (UHV) compatible in order to assure a background pressure of $\leq10^{-8}$ mbar. Ultrapure hydrogen (99.9999%) (Messer Griesheim) with Oxysorb purifying cartridge, which reduces the total oxygen and water content below 1 ppm, was used as the process gas at a flow rate of 0.3 mbar l/s during the etching.

The Si sample was cleaned using the RCA procedure[70] followed by about a 30 s dip in diluted HF/H_2O acid, which left a clean hydrophobic surface passivated by chemisorbed hydrogen.[71] The sample holder was screened by an electrically insulating silica tube so that only the Si-sample surface of about 1.6 cm^2 area was exposed to the plasma. Prior to the etching experiment, the whole discharge tube was thermally isolated and a higher hydrogen flow rate was set as to obtain a pressure of about 1 mbar in the discharge tube. A discharge current of about 1 A was used in order to clean the whole system. The temperature of the sample was set to 500 °C. Under these conditions, the temperature of the discharge tube reached ≥300 °C and the surface of the inner walls was reduced to almost pure silicon, which reduced the desorption of oxygen-containing species during the subsequent etch experiment. After ≥15 h, the cleaning was stopped, the thermal insulation was removed, and the discharge tube was cooled with water. Under these conditions, the total desorption and leak rate was about 5×10^{-6} mbar l/s. The total background pressure was about 2×10^{-7} mbar and was dominated by hydrogen desorbing from the walls due to the "hydrogen recycling," which is well known, e.g., from the Tokamak devices for controlled nuclear fusion.[63,72] Thus, the total oxygen impurity content in the hydrogen plasma was $\leq2-3$ ppm, as determined by calibrated quadrupole-mass spectrometry when introducing oxygen through the UHV leak valve and adjusting its pressure in the discharge tube, which was measured by an absolute pressure gauge (Baratron).

The electrical bias of the sample with respect to the surrounding plasma was determined in the following way: The current flowing to the Si sample was measured as a function of the voltage applied between the sample and the ground. When the current reached the value of 0, the voltage corresponded to the local "wall potential" (or "floating") where the fluxes of electrons and low energy ions just cancel each other.[73,74] The floating potential was about 10–15 V negative with respect to the potential of the surrounding plasma, and the energy of the ions reaching the sample surface of about 10 to 15 V was clearly under the threshold for physical sputtering under these conditions (see Fig. 4.8 in Ref. 75, p. 169). The required negative bias of the sample was then adjusted with respect to this reference "floating" potential by means of the auxiliary bias unit.

The etch rate was determined from the weight loss of the sample using an ultra-microbalance with accuracy of

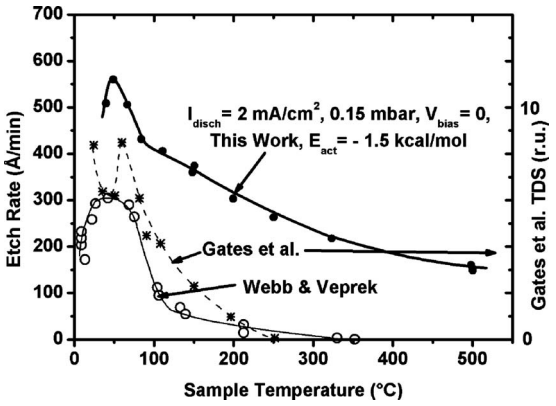

FIG. 2. Etch rate as a function of the temperature of the Si sample at discharge current density $I_{disch}=2$ mA/cm^2, hydrogen pressure of 0.15 mbar, and floating potential $V_{bias}=0$ V. The results of Webb and Veprek and Gates *et al.* are shown for comparison (see text).

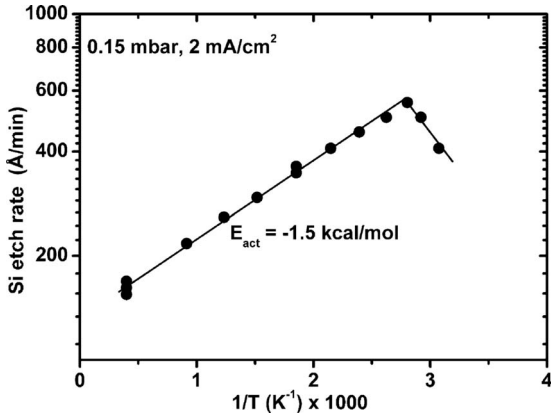

FIG. 4. Arrhenius plot of the etch rate vs reciprocal temperature.

0.1 μg. The relatively small weight loss during the cleaning with the sample at high temperature was determined several times and, because it was well reproducible, it was subtracted from the total weight loss during the cleaning and subsequent etching in order to obtain the actual etch rate in the experiment. With the etched area of 1.6 cm^2, the accuracy of the etch rate was about 3 Å/τ, where τ is the time of etching, typically of $\geq$100 min. In some experiments, the etch rate was determined from the intensity of the SiH_2^+ signal in the quadrupole-mass spectrometer, which was connected to the discharge tube via a small orifice and differentially pumped with a separate turbo-pump (not shown in Fig. 1). For this purpose, the intensity of the signal was calibrated versus the etch rate determined by the weight loss.

III. RESULTS AND DISCUSSION

A. Etching of silicon in pure hydrogen plasma

In this subsection, we present results obtained in pure hydrogen plasma where the oxygen impurity was less than 2–3 ppm. Figure 2 shows the etch rate versus sample temperature as obtained in the present work at floating potential under the conditions specified in the figure. The results of Webb and Veprek[53] and of Gates *et al.*[66] are shown for comparison. The higher etch rate obtained in the present work as compared with Webb and Veprek is due to the higher concentration of atomic hydrogen, which is the result of a larger diameter of the discharge tube and higher discharge-current density.

This is semiquantitatively shown in Fig. 3 where the etch rate is plotted as a function of discharge-current density. For small current, the density of H atoms increases approximately linearly with the current, changing to a sublinear dependence at medium currents due to complex processes of dissociation and recombination. One notices also the good agreement between the etch rate measured by weight loss and by calibrated-mass spectrometry.

Figure 4 shows the Arrhenius plot of the etch rate versus reciprocal temperature. For temperatures below the maximum etch rate, the activation energy is positive. At higher temperatures, the activation energy is negative of about −1.5 kcal/mol. This is less than the value of −4.5 kcal/mol found by Veprek and Sarott during the electron-induced etching in hydrogen plasma[55] but close to the value of −1.6 kcal/mol reported by Abrefah and Olander for etching of silicon with thermally produced H atoms.[65] The present results are in accord with the reaction mechanism that has been suggested by Veprek and Sarott[55] and by Abrefah and Olander[65] and is shown schematically in Fig. 5.

Abrefah and Olander also considered diffusion of hydrogen into the silicon. This is not included in the present, simplified mechanism because, due to the very high, time-independent fluxes of atomic hydrogen of the order of

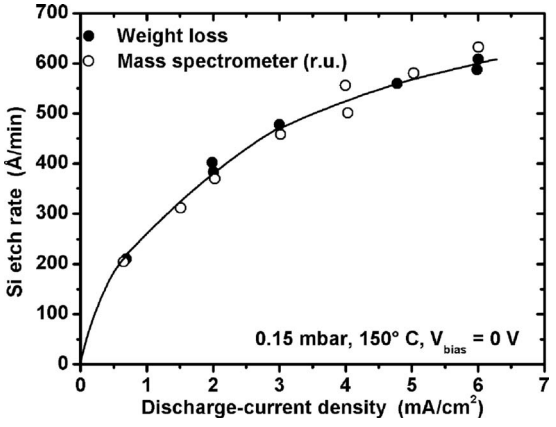

FIG. 3. Dependence of the etch rate on discharge-current density at floating potential and temperature of the Si sample of 150 °C.

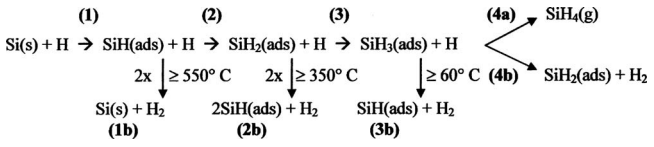

FIG. 5. Simplified reaction mechanism (see text).

10^{19} atoms/cm^2 s in our work, as compared to about 10^{16} atoms/cm^2 s in the work of Abrefah and Olander, the hydrogen concentration in our sample reaches a steady state after a relatively short time, as compared to the time of the etching.

All the authors[53,55,65] agreed, and Gates *et al.*[66–69] confirmed in very detailed experiments, that for an efficient etching, a high surface concentration of the SiH_3 groups is necessary in order to enable the formation of SiH_4 in step 4a (see Fig. 5). The initial, small increase of the etch rate with temperature (below about 60 °C) is due to the thermally activated formation of the final SiH_4 product (step 4a in Fig. 5), whereas its decrease is due to the competing recombination and release of H_2 by all possible reactions (H-abstraction step 4b and heterogeneous recombinations steps 3b, 2b, and 1b). The activation energy of the silane formation (step 4a in Fig. 5) of 10 kcal/mol estimated by Veprek and Sarott for electron-induced etching with hydrogen and of 1.8 kcal/mol found by Abrefah and Olander in molecular beam experiment are in reasonable agreement if one takes into account the significantly different experimental conditions, where the fluxes of atomic hydrogen differed by orders of magnitude. The competing hydrogen abstraction (step 4b) should have activation energy of about 3–4 kcal/mol by analogy with its gas-phase counterparts $SiH_4(g)+H(g)\rightarrow SiH_3+H_2$,[76] because in both cases it involves the same step of breaking a Si-H bond whose energy depends only slightly on the number of Si-H bonds in SiH_x, $x\geq 3$. Only slightly higher values were reported for hydrogen abstraction from hydrocarbons, which is in agreement with the stronger C-H bond.[77]

The recombination of chemisorbed hydrogen and desorption of H_2 from the SiH_y, $y\leq 3$, surface groups according to steps 1b, 2b, and 3b in Fig. 5 occurs at different temperatures. Their importance in the overall reaction mechanism depends on the surface coverage, which in turn is determined by a balance between the flux of H atoms and the temperature. As already mentioned, the fluxes are orders of magnitude higher in our earlier papers and especially in the present work, as compared with those in the modulated-beam experiment of Abrefah and Olander, and in the adsorption/desorption experiments of Gates *et al.* Nevertheless, some general trends can be summarized which are in agreement with all the papers on this subject: The SiH_3 groups already start decomposing to SiH(ads) and H_2 below 50 °C with activation energy of about 2 kcal/mol, and no SiH_3 could be detected at 400 °C in the "static" experiment of Gates *et al.*[69] For the Si surface saturated with chemisorbed hydrogen the SiH_3(ads) species can be still detected at a somewhat higher temperature of 402 °C.[67,69]

Many papers have shown that upon annealing with a linear temperature increase under ultra-high vacuum (UHV), a silicon surface, which was originally fully saturated with hydrogen, will release H_2 from the SiH_3 and SiH_2 groups with a maximum desorption rate at about 350 °C, leaving the monohydride phase Si-H(ads) (e.g., Refs. 66–69 and 78). Only above 550 °C does this monohydride phase release H_2 due to heterogeneous recombination $2SiH(ads)\rightarrow Si(s)+H_2$. In general, the activation energy of any of the steps releasing H_2 in Fig. 5 will also depend to some extent on the surface coverage due to the adsorbate-adsorbate interaction. Therefore, the activation energies for the overall desorption of H_2 of 2.8 kcal/mol (Ref. 55) and of 4.5 kcal/mol (Ref. 65) are in a reasonable agreement with the other published data.

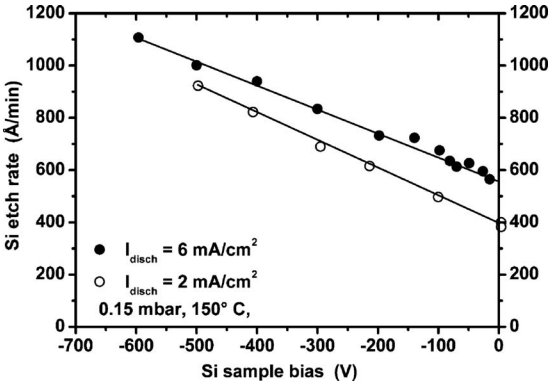

FIG. 6. Effect of substrate bias on silicon etching at a pressure of 0.15 mbar, sample temperature of 150 °C, and two different discharge-current densities of 2 and 6 mA/cm^2.

When the Si surface is exposed to an intense, clean hydrogen plasma where the H atom flux reaches $\geq 10^{19}$ H atoms/cm^2 s, the mono- and polyhydride phases can be stabilized at much higher temperature[71,79] depending on the flux of the H atoms.[53] This explains why, in the present paper, we still find a measurable high etch rate even at the temperature of 500 °C, whereas in the work of Webb and Veprek, and Gates *et al.*, the etch rates decreased below the detection limit (see Fig. 2). Obviously, the higher the flux of H atoms toward the Si surface, the higher the etch rate and the slower is its decrease with increasing temperature above the optimum value of 60–70 °C.

Increasing the substrate bias slightly increases the etch rate (see Fig. 6). This might be due to subplantation of hydrogen, momentum-transfer-enhanced mixing and diffusion within the hydrogenated surface layer,[47] or ion-induced chemical sputtering.[46] Physical sputtering can be ruled out because, when using the published values of the sputter yield[75] and the measured ion flux, and assuming that the ions have energy corresponding to the value of the bias (an overestimate), the maximum contribution of physical sputtering may be of 2–4 Å/min, which is negligible as compared with the measured etch rate shown in Fig. 6. The experimental results presented in Fig. 6 will be useful for the understanding of the mechanism of anisotropic etching later in this paper.

Veprek and Sarott reported roughening of the Si surface upon etching with hydrogen under electron bombardment (see Figs. 5 and 6 in Ref. 55). Also, Abrefah and Olander found surface roughening (see Fig. 4 in Ref. 65). Figure 7 shows examples of the surface morphology of a Si sample etched in clean hydrogen plasma at 150 °C and bias of −150 V. The morphology is typical of crystallographic etch-

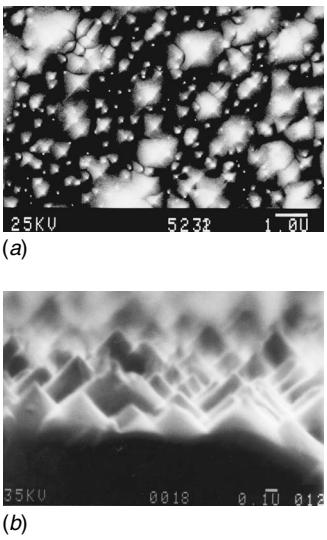

FIG. 7. Scanning electron micrographs (SEMs) showing example of the surface morphology of Si sample etched in clean hydrogen plasma at a pressure of 0.15 mbar, temperature of 150 °C, and bias −150 V. (a) is top view and (b) is a side view under glancing incidence.

ing. A series of detailed studies has shown that the roughness increases with increasing sample temperature and decreasing negative bias. Samples etched at a temperature close to the maximum etch rate (e.g., 80 °C) and negative bias of −150 V or more have fairly flat surfaces. We do not show these details here because they are not of much importance in the context of this work.

B. Effect of oxygen impurities

In this series of experiments, ultra-pure oxygen (99.999%) was added into the hydrogen discharge via a UHV leak valve and its concentration in the gas phase was measured by means of calibrated quadrupole-mass spectrometer. The results are shown in Fig. 8 for the Si sample at

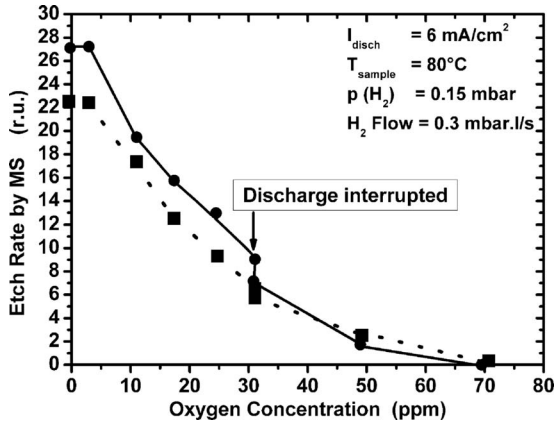

FIG. 8. Effect of the addition of oxygen impurities on the etch rate of silicon in contaminated hydrogen plasma at a sample temperature of 80 °C, total pressure of 0.15 mbar, and a relatively high discharge current density of 6 mA/cm^2 and sample bias of 0 V. The different symbols (squares and full circles) correspond to two successive experiments.

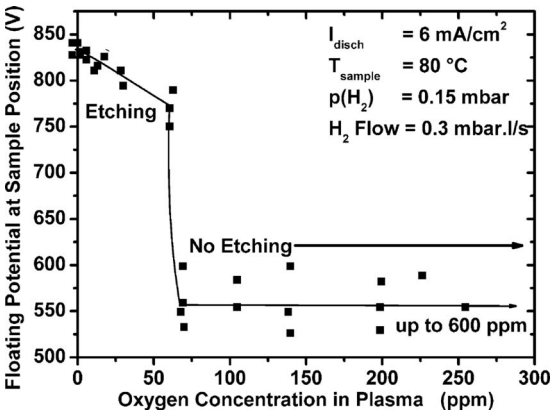

FIG. 9. Effect of oxygen concentration on the value of the floating potential with respect to the grounded cathode (see text).

floating potential and two different experimental runs (squares and circles) in order to demonstrate the reproducibility. Notice that the temperature of the sample was kept at 80 °C where the etch rate in pure hydrogen plasma is close to maximum (see Fig. 2). In order to assure constant conditions and to save time, the etch rate was measured *in situ* by means of the calibrated mass spectrometry. During the measurement, the discharge was interrupted at oxygen concentration of 30 ppm in order to illustrate the effect of increasing contamination of the surface of the Si sample in the absence of plasma.

One can see that already 10 ppm of oxygen impurities noticeably reduced the etch rate and, at an oxygen concentration of more than 70 ppm, the etch rate stops. This is due to formation of a thin oxide layer on the surface of the Si sample, which prevents the silicon etching by hydrogen. We shall see in the next section that, indeed, silica cannot be etched at temperatures below 300 °C.

With increased oxygen-impurity content, the floating potential, measured with respect to the grounded cathode (see Fig. 1), also decreased almost linearly, and at a concentration of about 70 ppm, when the etching stops, a sharp decrease of about 200 V was seen (see Fig. 9). With a further increase of oxygen impurity, the floating potential remained essentially constant up to the upper limit of 600 ppm measured in this work. This can be qualitatively understood in terms of the higher ionization energy of H_2 as compared with O_2 (Ref. 80) and due to the fact that pure hydrogen (and silane) discharge has a relatively high axial-field strength because of electron energy losses by excitation of molecular vibrations.[73] Extensive theoretical modeling of the glow discharge would be necessary in order to quantify this effect theoretically. We do not attempt to do that. This example only illustrates the consistency with the etching results.

The decrease of the etch rate with increasing oxygen impurities was due to the formation of the SiO_x surface layer which acts as a barrier for hydrogen, which cannot chemisorb on the underlying Si surface and facilitate the etching according to mechanism summarized in Fig. 5. SiO_2 can be etched in hydrogen discharge only at a high temperature of

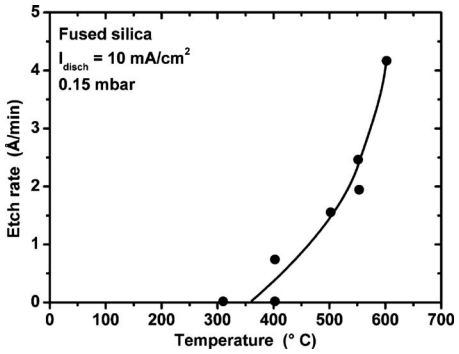

FIG. 10. Temperature dependence of the etch rate of SiO_2 in pure hydrogen plasma at pressure of 0.15 mbar and a relatively high discharge current density of 10 mA/cm^2.

$\geq$350 °C where, as seen in Fig. 2, the etching of Si by atomic hydrogen either stops (see Refs. 53 and 66) or strongly decreases (present work). Thus, a selective etching of Si and SiO_2 should be possible by means of the control of the temperature.

C. Etching of SiO_2

Silicon dioxide cannot be etched with molecular hydrogen below about 1200 °C because the chemical equilibrium of both reactions (1a) and (1b) is strongly shifted to the left-hand side, with Gibbs free energy of the reactions (1a) and (1b) at 873 °C of +372 and +433 kJ/mol, respectively. Notice that reaction (1a) corresponds to reduction of the silica whereas (1b) corresponds to etching. The values of the Gíbbs free energy of the formation of the reactants and products were taken from[81]

$$SiO_2(s) + 2H_2 = Si(s) + 2H_2O(g), \quad (1a)$$

$$SiO_2(s) + H_2 = SiO(g) + H_2O(g). \quad (1b)$$

In the hydrogen-glow discharge with a concentration of atomic hydrogen of several vol. %, we consider, as a simplified case, reactions (2a) and (2b). The corresponding Gibbs free energies of these reactions at 873 °C are −378.4 and +57.8 kJ/mol, respectively. This means that with atomic hydrogen, the reduction of the silica surface to Si [reaction (2a)] and a subsequent formation of silanes can occur, whereas the etching according to reaction (2b) cannot proceed:

$$SiO_2(s) + 4H = Si(s) + 2H_2O(g), \quad (2a)$$

$$SiO_2(s) + 2H = SiO(g) + H_2O(g). \quad (2b)$$

Webb and Veprek reported that the etching of silica in hydrogen plasma commences above 400 °C, and at 450 °C reaches about 30 Å/min.[82] This is in fair agreement with the results of the present study, which are shown in Fig. 10.

For given conditions, the etch rate increased with increasing discharge-current density. The Arrhenius plot of the logarithm of the etch rate versus reciprocal temperature yields a straight line with activation energy of +10 kcal/mol (not shown here). This is much less than the activation energy of 90 kcal/mol reported for the disproportionation reaction $SiO_2(s) + Si(s) \rightarrow 2SiO(g)$ and sublimation of SiO.[83–86] The volatility of $SiO(g)$ at elevated temperatures is used during silicon-microelectronic processing in order to clean the Si surface covered with oxide via the disproportionation reaction, which is usually carried on at a high temperature of $\geq$1000 °C. Earlier studies by one of the authors have shown that exposure of silica to hydrogen plasma at $\geq$1000 °C results in the formation of a sufficiently large quantity of $SiO(g)$ to convert about 10 mg of barium titanate, $BaTiO_3$, to barium sphene, $BaTiSiO_5$, within 1 h.[87] This is consistent with the volatility of SiO, which is very low at 400 °C, but sufficient at 1000 °C.[81] Considering the equilibrium pressure of SiO at about 400 °C reported in Ref. 81 (see p. 1650), the expected desorption rate of SiO should be of the order of $c_v \times 10^4$ molecules/cm^2 s ($c_v < 1$ is the vaporization coefficient), which is orders of magnitude lower than the measured etch rate of about 1 Å/min reported in Fig. 10, which would correspond to more than 1×10^{14} SiO molecules/cm^2 s. Based on these results, we can rule reaction (2b) out.

The onset of the etching of SiO_2 at about 350 °C and its strong increase with increasing temperature is consistent with desorption of chemisorbed water on silica from isolated silanol groups.[88,89] Because the etch rate of silicon at 400 °C in pure hydrogen is almost 200 Å/s, the most likely etch mechanism of silica etching in hydrogen plasma is the reduction of SiO_2 to Si according to reaction (2a) with thermally induced desorption of water from the silanol groups, followed by subsequent formation of silane according to the scheme in Fig. 5. The mass-spectrometric signal of SiH_2^+ observed during the etching is consistent with this suggestion.

D. Control of the isotropic versus anisotropic etching

For this study, Si samples were patterned with chromium masks using contact lithography and the lift-off technique with a feature size of several μm. (Note that the conventional photoresist, which would allow us to demonstrate etching of smaller feature sizes, could not be used because it would be etched away by the intense hydrogen plasma. One may, of course, use another inorganic resist, which can sustain the attack by atomic hydrogen, but this technique was not available to us.) In pure hydrogen plasma, the etching was almost isotropic, as illustrated in Fig. 11(a). The undercut and overetching resulted in a collapse and loss of the mask in many parts of the etched sample. The addition of a small amount of oxygen and the simultaneous application of negative bias resulted in anisotropic etching, as illustrated in Fig. 11(b). One can clearly see the perpendicular sidewalls, which illustrates the high degree of anisotropy that can be achieved under the given conditions.

In order to elucidate the mechanism responsible for the anisotropic etching, we show in Fig. 12 the dependence of the degree of anisotropy, defined as the ratio of the vertical to horizontal etch rate calculated from scanning electron micrographs (see the y-axis on the right-hand side), for hydrogen

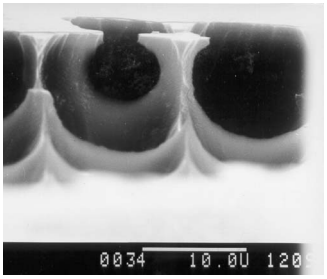

(*a*)

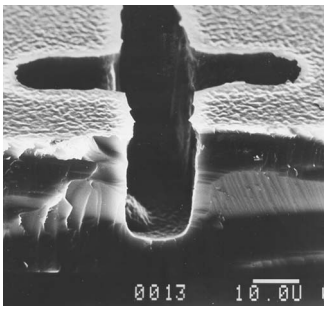

(*b*)

FIG. 11. (a) Example of an almost isotropic etching of patterned Si wafer in pure hydrogen plasma. $V_{bias}=0$ V. (b) Example of anisotropic etching upon addition of 4–7 ppm of oxygen and applying negative bias of −300 V. Sample temperature 73 °C, discharge current density 6 mA/cm^2, and pressure 0.15 mbar.

contaminated with oxygen impurities similar to Fig. 11(b), and the ratio of etch rate in pure hydrogen at a given negative bias to that at floating potential (see *y*-axis on the left-hand side in Fig. 12). Because the increase of anisotropy with increasing negative bias in oxygen-contaminated discharge is significantly stronger than that of the etch rates in pure hydrogen discharge, it is clear that the anisotropy is due to the passivation of side-walls by a very thin oxide film. The oxide contamination was removed from the bottom surface by the ion bombardment, which enabled its etching with atomic hydrogen.

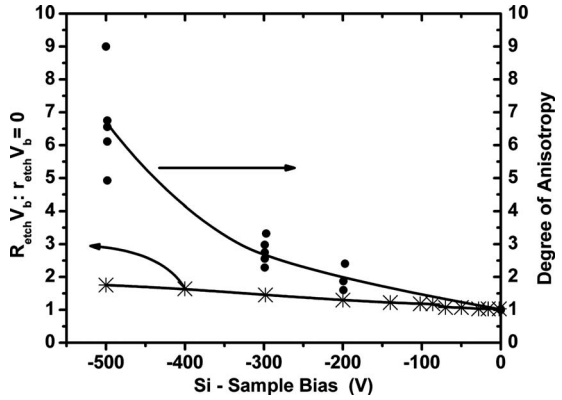

FIG. 12. Effect of the bias on the degree of anisotropy in oxygen-contaminated plasma and the ratio of the etch rate under the given bias to that at floating potential in a clean hydrogen plasma. Conditions as in Fig. 11, only the somewhat higher temperature of 150 °C was chosen in order to obtain better reproducibility.

IV. CONCLUSIONS

The etching of silicon in a hydrogen-glow discharge is reproducible and efficient only when the oxygen impurity content in the plasma is 3–5 ppm or less. Higher oxygen content strongly reduces the etch rate due to formation of surface oxide. Application of negative bias helps to remove the oxide layer by ion bombardment and to etch the underlying silicon. However, the etching is less efficient than in pure hydrogen plasma. Oxygen impurities in hot-wire processes will have the same detrimental effect.

In clean hydrogen plasma, the optimum temperature for the etching at high rates is between about 60 °C and 70 °C. The optimum temperature increases slightly with increasing concentration of atomic hydrogen, i.e., with increasing plasma density.

This process is of scientific interest and is also useful for the cleaning of discharge equipment contaminated with silicon (and Ge, P, As, …) deposits. Because such deposits are likely to be contaminated with oxygen, energetic ion bombardment at a bias of 100–300 V, dense plasmas, and somewhat higher temperature of 120–150 °C are suitable in order to achieve efficient removal of the contaminants and a sufficient etch rate of silicon.

In clean hydrogen plasma, the etching is isotropic. The addition of a small amount of oxygen impurities in the range of ≤ 10 ppm and the simultaneous application of negative bias to the etched Si sample allows one to control the anisotropy within a wide range.

The silicon etching and patterning with hydrogen plasma, as demonstrated in this paper, is of limited interest to microelectronic technology because of complex electronic effects of hydrogen dissolved in the silicon wafer, and also because of the hydrogen embrittlement. For the same reasons, cleaning of silicon wafers by atomic hydrogen will results in similar undesirable damage of the silicon material.

[1] M.-C. Chuang and J. Coburn, J. Vac. Sci. Technol. A **8**, 1969 (1990).
[2] W. Beyer, M. Lejeune, J. Müller, U. Zsattrow, M. Albert, and T. Rößler, Proc. 3rd World Conf. on Photovoltaic Energy Conversion, Osaka, 11–18 May 2003, p. 1584.
[3] M. Ishii, K. Nakashima, T. Hayakawa, I. Tajima, and M. Yamamoto, J. Vac. Sci. Technol. B **12**, 2342 (1994).
[4] Y. Wei, L. Li, and S. T. Tsong, Appl. Phys. Lett. **66**, 1818 (1995).
[5] H. P. Gillis, D. A. Choutov, P. A. Steiner IV, J. D. Piper, J. H. Crouch, P. M. Dove, and K. P. Martin, Appl. Phys. Lett. **66**, 2475 (1995).
[6] I. Kaiser, N. H. Nickel, and W. Fuhs, Phys. Rev. B **58**, R1718 (1998).
[7] K. Saitoh, M. Kondo, M. Fukawa, T. Nishimiya, A. Matsuda, W. Futako, and I. Shimizu, Appl. Phys. Lett. **71**, 3403 (1997).
[8] C. Summonte, R. Rizzoli, A. Desalvo, F. Zignani, E. Centurioni, R. Pinguini, and M. Gemmi, J. Non-Cryst. Solids **266–269**, 624 (2000).
[9] S. Sriraman, M. S. Valipa, E. S. Aydil, and D. Maroudas, J. Appl. Phys. **100**, 053514 (2006).
[10] S. Agarwal, A. Takano, M. C. M. van de Sanden, D. Maroudas, and E. S. Aydil, J. Chem. Phys. **117**, 10805 (2002).
[11] A. Matsuda, J. Non-Cryst. Solids **338–340**, 1 (2004).
[12] K. Nomoto, Y. Urano, J. L. Guizot, G. Gabguly, and A. Matsuda, Jpn. J. Appl. Phys., Part 2 **29**, L1372 (1990).
[13] D. Das and K. Bhattacharya, J. Appl. Phys. **100**, 103701 (2006).

[14]T. Kamei, Appl. Phys. Lett. **89**, 262121 (2006).
[15]A. Fontcuberta i Morral and P. Roca i Cabarrocas, Eur. J. Appl. Physiol. **35**, 165 (2006).
[16]E. A. G. Hamers, A. Fontcuberta i Morral, C. Niikura, R. Brenot, and P. Roca i Cabarroca, J. Appl. Phys. **88**, 3674 (2000).
[17]T. Zecho, B. D. Brandner, J. Biener, and J. Küppers, J. Phys. Chem. B **105**, 3502 (2001).
[18]H. N. Wanka and M. B. Schubert, J. Phys. D **30**, L28 (1997).
[19]R. P. H. Chang, C. C. Chang, and S. Darack, J. Vac. Sci. Technol. **20**, 45 (1982).
[20]B. Anthony, L. Breaux, T. Hsu, S. Banerjee, and A. Tasch, J. Vac. Sci. Technol. B **7**, 621 (1989).
[21]R. A. Rudder, S. V. Hattangady, J. B. Posthill, and R. J. Markunas, Mater. Res. Soc. Symp. Proc. **116**, 529 (1988).
[22]T. Shibata, N. Kondo, and Y. Nanishi, J. Electrochem. Soc. **136**, 3459 (1989).
[23]I. Suemune, Y. Kunitsugu, Y. Kan, and M. Yamanishi, Appl. Phys. Lett. **55**, 760 (1989).
[24]T. Hsu, B. Anthony, R. Qian, J. Irby, S. Banerjee, A. Tasch, S. Liu, H. Marcus, and C. Magee, J. Electron. Mater. **20**, 279 (1991).
[25]M. Ishii, K. Nakashima, I. Tajima, and M. Yamamoto, Appl. Phys. Lett. **58**, 1378 (1991).
[26]P. Raynaud, J. P. Booth, and C. Pomot, Appl. Surf. Sci. **46**, 435 (1990).
[27]B. Anthony, T. Hsu, L. Breaux, R. Qian, S. Banerjee, and A. Tasch, J. Electron. Mater. **19**, 1027 (1990).
[28]Y. Okada, H. Shimomura, T. Sugaya, and M. Kawabe, Jpn. J. Appl. Phys., Part 1 **30**, 3774 (1991).
[29]T. Hsu, B. Anthony, R. Qian, J. Irby, D. Kinosky, A. Mahajan, S. Banerjee, C. Magee, and A. Tasch, J. Electron. Mater. **21**, 65 (1992).
[30]M. Delfino, S. Salimian, D. Hodul, A. Ellingboe, and W. Tsai, J. Appl. Phys. **71**, 1001 (1992).
[31]R. R. Burke, J. Pelletier, C. Pomot, and L. Vallier, J. Vac. Sci. Technol. A **8**, 2931 (1990).
[32]A. Sherman, J. Vac. Sci. Technol. B **8**, 656 (1990).
[33]H. Iwakuro, T. Inoue, and T. Kuroda, Jpn. J. Appl. Phys., Part 2 **30**, L255 (1991).
[34]G. G. Fountain, R. A. Rudder, S. V. Hattangady, R. J. Markunas, and P. S. Lindorme, J. Appl. Phys. **63**, 4744 (1988).
[35]M. Hirose, T. Yasaka, M. Takakura, and S. Miyazaki, Solid State Technol. **34**, 43 (1991).
[36]J. Ramm, E. Beck, and A. Zueger, Mater. Res. Soc. Symp. Proc. **220**, 15 (1991).
[37]J. Ramm, E. Beck, A. Zueger, A. Dommann, and R. E. Pixley, Thin Solid Films **222**, 126 (1992).
[38]H. F. Dylla, S. A. Cohen, S. M. Rossnagel, G. M. McCracken, and P. Staib, J. Vac. Sci. Technol. A **6**, 1276 (1988).
[39]W. Poschenrieder, G. Standenmaier, and P. Staib, J. Nucl. Mater. **93-94**, 322 (1980).
[40]S. Veprek and V. Marecek, Solid-State Electron. **11**, 683 (1968).
[41]A. V. Shah, J. Meier, E. Vallat-Sauvain, N. Wyrsch, U. Kroll, C. Droz, and U. Graf, Sol. Energy Mater. Sol. Cells **78**, 469 (2003).
[42]S. Klein, F. Finger, R. Carius, and M. Stutzmann, J. Appl. Phys. **98**, 024905 (2005).
[43]S. W. Ing and Y. S. Chiang, J. Electrochem. Soc. **113**, 192 (1966).
[44]A. R. Reinberg, in *Plasma Etching*, edited by D. M. Manos and D. L. Flamm (Academic, Harcout Brace Jovanovic, Boston, 1989).
[45]D. L. Flamm, in *Plasma Etching*, edited by D. M. Manos and D. L. Flamm (Academic, Harcout Brace Jovanovic, Boston, 1989).
[46]*Sputtering by Particle Bombardment, Vol. I – III*, edited by R. Behrisch (Springer Verlag, Berlin, 1981, 1983, 1991).
[47]H. F. Winters, in *Plasma Chemistry III*, edited by S. Veprek and M. Venugopalan (Springer-Verlag, Berlin, 1980).
[48]A. Güntherschulze, Z. Phys. **36**, 563 (1926).
[49]S. Veprek and H. R. Oswald, Z. Anorg. Allg. Chem. **415**, 190 (1975).
[50]W. E. Spear, P. G. Le Comber, S. Veprek, and R. Wild, Philos. Mag. **38**, 349 (1978).
[51]J. Brunner, M. Thüler, S. Veprek, and R. Wild, Helv. Phys. Acta **51**, 461 (1978).
[52]S. Veprek, A. P. Webb, H. R. Oswald, and H. Stuessi, J. Nucl. Mater. **68**, 32 (1977).
[53]A. P. Webb and S. Veprek, Chem. Phys. Lett. **62**, 173 (1979).
[54]K. J. Leidler, *Chemical Kinetics*, 3rd ed. (Harper & Row, New York, 1987).
[55]S. Veprek and F.-A. Sarott, Plasma Chem. Plasma Process. **2**, 233 (1982).
[56]N. M. Johnson, Phys. Rev. B **31**, 5525 (1985).
[57]N. M. Johnson, Appl. Phys. Lett. **47**, 874 (1985).
[58]C. T. Shah, in *Properties of Silicon* (INSPEC, The Institution of Electrical Engineers, Gresham Press, Surrey, 1988), pp. 584–612.
[59]K. V. Ravi, in *Properties of Silicon* (INSPEC, The Institution of Electrical Engineers, Gresham Press, Surrey, 1988), pp. 918–920.
[60]C. Herring, N. M. Johnson, and C. G. Van de Walle, Phys. Rev. B **64**, 125209 (2001).
[61]S. Veprek, M. D. Wiggins, and R. Gotthardt, J. Nucl. Mater. **140**, 28 (1986).
[62]K. Yamashita, J. K. Gimzewski, and S. Veprek, J. Nucl. Mater. **128–129**, 705 (1984).
[63]S. Veprek, M. Kitajima, K. Yamashita, and P. Groner, J. Nucl. Mater. **128–129**, 636 (1984).
[64]T. Schober, H. Wenzl, and Ch. A. Wert, in *Hydrogen in Metals, Vol. II*, edited by G. Alefeld and J. Völkl (Springer-Verlag, Berlin, 1978).
[65]J. Abrefah and D. R. Olander, Surf. Sci. **209**, 291 (1989).
[66]S. M. Gates, R. R. Kunz, and C. M. Greenlief, Surf. Sci. **207**, 364 (1989).
[67]S. M. Gates, C. M. Greenlief, and D. B. Beach, J. Chem. Phys. **93**, 7493 (1990).
[68]C. M. Greenlief, S. M. Gates, and P. A. Holbert, Chem. Phys. Lett. **159**, 202 (1989).
[69]S. M. Gates, C. M. Greenlief, S. K. Kulkarni, and H. H. Sawin, J. Vac. Sci. Technol. A **8**, 2965 (1990).
[70]W. Kern and D. A. Puotinen, RCA Rev. **31**, 187 (1970).
[71]S. Veprek, F.-A. Sarott, S. Rambert, and E. Taglauer, J. Vac. Sci. Technol. A **7**, 2614 (1989).
[72]D. M. Gruen, S. Veprek, and R. B. Wright, in *Plasma Chemistry I*, edited by S. Veprek and M. Venugopalan (Springer Verlag, Berlin, 1980).
[73]A. von Engel, *Ionized Gases*, 2nd ed. (Clarendon, Oxford, 1965).
[74]B. Chapman, *Glow Discharge Processes: Sputtering and Plasma Etching* (Wiley, New York, 1980).
[75]H. H. Anderson and H. L. Bay, in *Sputtering by Particle Bombardment I*, edited by R. Behrisch (Springer Verlag, Berlin, 1981).
[76]K. Y. Choo, P. P. Gasper, and A. P. Wolf, J. Phys. Chem. **79**, 1752 (1975).
[77]A. F. Trorman-Dickenson and G. S. Milne, *Tables of Bimolecular Gas Reactions, National Standard Reference Data Series* (National Bureau of Standards, Washington, DC, 1967).
[78]G. Schulze and M. Henzler, Surf. Sci. **124**, 336 (1983).
[79]P. Raynaud, J. P. Booth, and C. Pomot, Appl. Surf. Sci. **46**, 435 (1990).
[80]J. B. Hasted, *Physics of Atomic Collisions* (Butterworths, London, 1972).
[81]M. W. Chase, C. A. Davies, J. R. Downey, D. J. Frurip, R. A. McDonald, and A. N. Syverud, *JANAF Thermochemical Tables, 3rd. edition*, J. Phys. Chem. Ref. Data 14 (1985), Supplement 1.
[82]S. Veprek and A. P. Webb, Proc. Int. Symp. Plasma Chem., University of Zurich, 1979, p. 79.
[83]M. P. D'evelyn, M. M. Nelson, and T. Engel, Surf. Sci. **186**, 75 (1987).
[84]J. R. Engstrom, M. M. Nelson, and T. Engel, J. Vac. Sci. Technol. A **7**, 1837 (1989).
[85]J. R. Engstrom and T. Engel, Phys. Rev. B **41**, 1038 (1990).
[86]J. R. Engstrom, D. J. Bonser, M. M. Nelson, and T. Engel, Surf. Sci. **256**, 317 (1991).
[87]H. Arend, S. Veprek, and J. Novak, Krist. Tech. **3**, K41 (1968).
[88]R. K. Iller, *The Chemistry of Silica* (Wiley, New York, 1979).
[89]L. T. Zhuralev, Pure Appl. Chem. **61**, 1060 (1991).